J Solid State Electrochem (2012) 16:1333–1341
DOI 10.1007/s10008-011-1528-z

ORIGINAL PAPER

Solid-contact Cu(II) ion-selective electrode based on 1,2-di-(*o*-salicylaldiminophenylthio)ethane

Slobodan Brinić · Marijo Buzuk · Marija Bralić · Eni Generalić

Received: 23 December 2010 / Revised: 2 August 2011 / Accepted: 8 August 2011 / Published online: 25 August 2011

Abstract The development of Cu(II) solid-contact ion-selective electrodes, based on 1,2-di-(*o*-salicylaldiminophenylthio)ethane as a neutral carrier, is presented. For the electrodes construction, unmodified carbon ink (type 1 electrode) and polymer membrane-modified carbon ink (type 2 electrode) were used as solid support and transducer layer. Also, carbon ink composite polymer membrane electrode (type 3 electrode) was prepared. The analytical performance of the electrodes was evaluated with potentiometry, while bulk and interfacial electrode features were provided with electrochemical impedance spectroscopy. It is shown that modification of carbon ink with polymer membrane cocktail decreases the bulk contact resistance of the transducer layer and polymer membrane, thus enhancing the analytical performance of the electrode in terms of sensitivity, linear range, and stability of potential. The optimized electrodes of types 2 and 3 exhibit a wide linear range with detection limits of 1.8×10^{-6} and 1.6×10^{-6} M, respectively. They are suitable for determination of Cu^{2+} in analytical measurements by direct potentiometry and in potentiometric titrations, within pH between 2.3 and 6.5. The electrodes are selective for Cu^{2+} over a large number of tested transition and heavy metal ions.

Keywords Cu(II) · ISE · Solid contact · Potentiometry · Impedance · Carbon ink

S. Brinić (✉) · M. Buzuk · M. Bralić · E. Generalić
Department of General and Inorganic Chemistry,
Faculty of Chemistry and Technology, University of Split,
Teslina 10/V,
21000 Split, Croatia
e-mail: brinic@ktf-split.hr

Introduction

Ion-selective electrodes (ISEs) are established tools that are capable of determining the activities of many analytes [1].

The new generation of ion-selective electrodes with internal solid contact has attracted much attention in the past decade due to their important advantages over conventional ISEs with internal solution [2].

In their original design [3, 4], a Pt wire was coated with a polymer membrane of usual composition. However, there were notable problems associated with the drift and overshoot of the standard potential, which have been mainly attributed to the lack of a thermodynamically well-defined electrochemical interface between the membrane and solid contact. To overcome these problems, adding an appropriate redox-active component in the membrane, such as a lipophilic silver complex [5], or use of conductive polymers as a contact between the solid support and membrane [6–10] was suggested.

Also, conductive polymers doped with redox-active species (e.g., hexacyanoferrate (II, III) ions) as ion-to-electron transducers have been used [11]. Furthermore, various intermediate layers have been described, including hydrogel [12] or redox-active self-assembled monolayers [13–15].

In recent years, ISEs have been composed of non-conductive organic polymers filled with electrical conductors, such as electrodes with graphite–epoxy intermediate layers [16–18] or electrodes with intermediate layers consisting of plasticizers-modified graphite paste [19]. In the fabrication of potentiometric electrodes, different forms of carbon paste electrodes [20] have been applied. Among others, conductive graphite-based polymer ink electrodes [21], carbon composite poly(vinyl

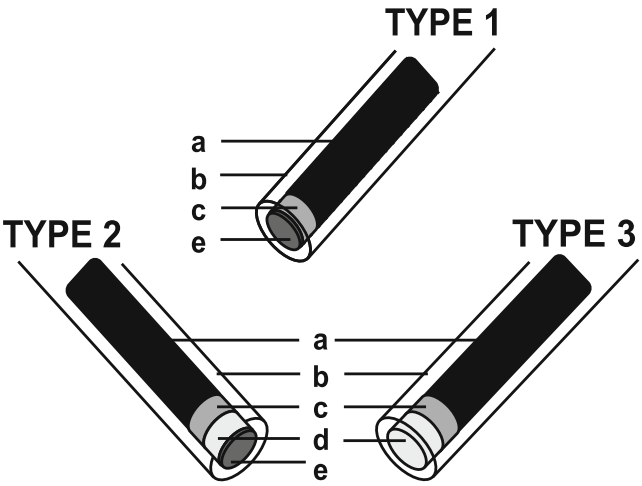

Fig. 1 Construction of the solid-contact ISE: graphite rod (**a**), PVC body (**b**), carbon ink (**c**), modified carbon ink (**d**), polymer membrane (**e**)

chloride) (PVC)-coated wire electrodes [21, 22], and PVC-modified screen-printed carbon paste electrodes [23–27] have been reported.

Nowadays, carbon nanotubes (CNTs), as solid transducer, standalone [28, 29] or combined with room temperature ionic liquids, as binders, have also been used for the preparation of the carbon paste electrodes [30–33].

Incorporation of nanosilica-based materials in CNT-modified carbon paste electrodes was reported [34–36], as well as application of self-assembled gold nanoparticles [37–40].

We have recently developed a conventional Cu(II) ion-selective electrode, with internal solution, using 1,2-di-(*o*-salicylaldiminophenylthio)ethane (SAPhTE) as ionophore [41]. The aim of this work was development of solid-contact ISE, characterized by a low-cost and simple preparation, with similar or even better response characteristics toward Cu(II) ions than the one reported [41]. As solid support and transducer layer, both unmodified and modified carbon ink (CI) were used; moreover, a carbon ink composite polymer–membrane electrode has been developed with SAPhTE as ionophore. The properties of the electrodes, besides potentiometric measurements, were examined by electrochemical impedance spectroscopy (EIS), which provided important information on membrane condition and sensor functionality.

Experimental

Ligand 1,2-di-(*o*-salicylaldiminophenylthio)ethane SAPhTE was synthesized as reported in [42] by adding an alcoholic solution of 1,2 di(o-aminophenylthio)ethane [42] (one molecular proportion) to an alcoholic solution of

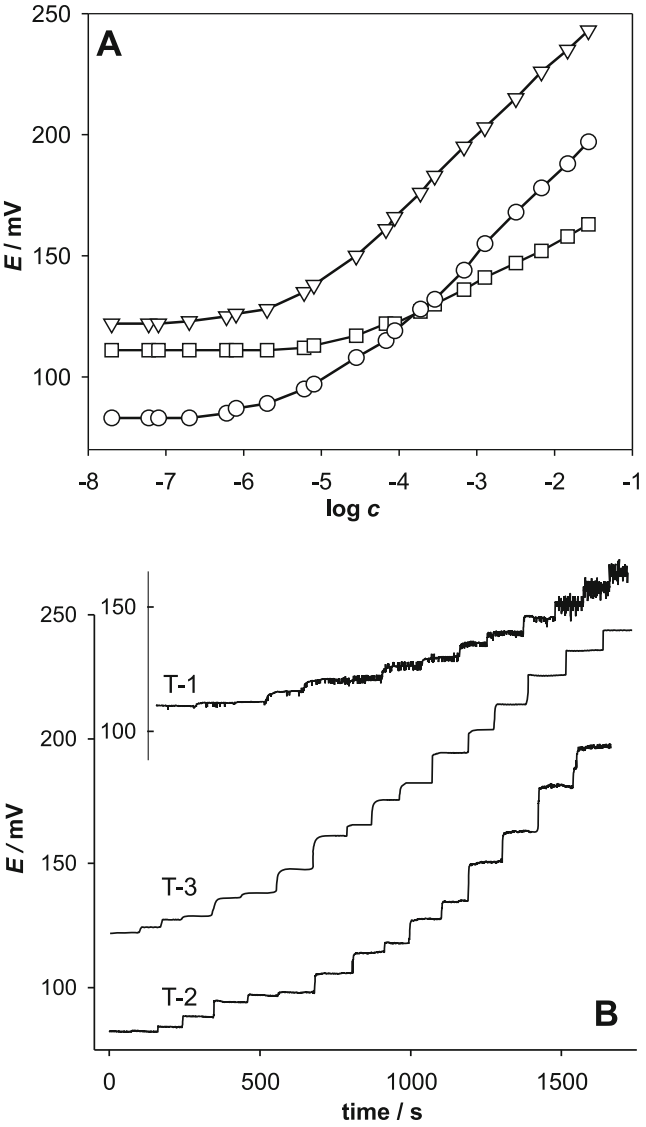

Fig. 2 Calibration curves (**a**) and dynamic responses (**b**) obtained by successive increases of Cu^{2+} concentration for different types of solid-contact ISE: T-1 (*unfilled squares*), T-2 (*unfilled circles*), T-3 (*unfilled inverted triangles*)

salicylaldehyde (two molecular proportions) in the presence of acetic acid.

Metallic potassium, absolute ethanol, salicylaldehyde, and 2-aminothiophenol were obtained from Fluka (Buchs,

Table 1 The potentiometric characteristics of optimized solid-contacts electrodes

Electrode	Slope (mV dec^{-1})	Linear range (M)	Detection limit (M)	pH range
T-1	16.5	3.0×10^{-5}–2.8×10^{-2}	2.5×10^{-5}	2.5–6.2
T-2	29.5	2.8×10^{-6}–2.8×10^{-2}	1.8×10^{-6}	2.3–6.5
T-3	31.0	3.2×10^{-6}–2.8×10^{-2}	1.6×10^{-6}	2.0–6.0

Switzerland). EDTA and dibromethane were obtained from Sigma Aldrich (St. Louis, MO, USA).

The membrane components, sodium tetraphenylborate (NaTPB), poly(vinyl chloride), dioctyl phthalate (DOP), and tetrahydrofuran (THF), were received from Fluka (Buchs, Switzerland). Membrane cocktail was prepared by dissolving 66 mg of PVC, 132 mg of plasticizer (DOP), 4 mg of SAPhTE, and 2 mg of NaTPB, as anionic additive, in 5 ml of THF and mechanically mixing the solution.

Preparation of the electrodes

Graphite rods (a) (6.1-mm diameter) were placed into home-made constructed PVC bodies (b) and cleaned by successive washing in acetone and THF, followed by ultrasonic treatment for 10 min in double-distilled water, and subsequently dried in air.

Three types of electrodes were constructed (see Fig. 1):

1. Type 1 (T-1): Graphite rod (a) was coated with 60 μl of carbon ink (c) (C50905DI, Gwent, Pontypol, UK) and allowed to dry for at least 48 h. The polymer membrane was deposited by solvent casting (3.0×20 μL) (e). Membrane cocktail, containing all components of the membrane in THF, was used for this purpose.
2. Type 2 (T-2): Graphite rod (a), modified with carbon ink (c), was coated with membrane cocktail-modified carbon ink (d). After drop-casting (60 μL), this layer was air-dried for 48 h. Further modification of the electrode was achieved by the solvent casting (3.0×20 μL) of membrane cocktail (e). The membrane cocktail-modified carbon ink layers (d) were prepared by mixing different ratios of carbon ink and membrane cocktail. These mixtures were homogenized by ultrasound for 5 min.
3. Type 3 (T-3): Construction of carbon ink composite polymer–membrane electrode was similar to the electrode type 2, except that this electrode was not coated with membrane cocktail (e).

An electrode with pure carbon ink (c), as blank electrode, was also prepared.

Table 2 Potentiometric characteristics of solid-contact T-2 electrodes for different compositions of the intermediate layer

Carbon ink (mg)	Membrane cocktail (ml)[a]	Slope (mV dec^{-1})	Linear range (M)	Detection limit (M)
50	1	23.0	5.0×10^{-5}–2.8×10^{-2}	4.0×10^{-5}
100	1	29.5	2.8×10^{-6}–2.8×10^{-2}	1.8×10^{-6}
150	1	19.3	8.0×10^{-5}–2.8×10^{-2}	6.0×10^{-5}

[a] Membrane cocktail composition: 66 mg of PVC, 132 mg of plasticizer (DOP), 4 mg of SAPhTE, and 2 mg of NaTPB; dissolved in 5 ml THF

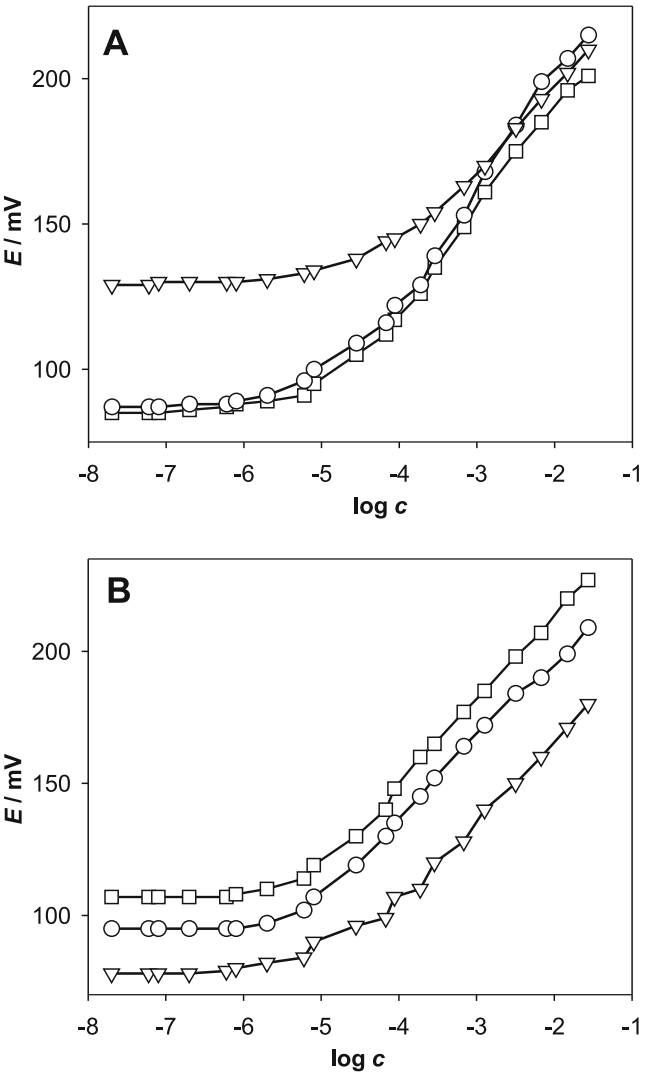

Fig. 3 The repeatability tests of potentiometric responses for the optimized T-2 electrode (**a**) and for the optimized T-3 electrode (**b**) after 7 days (*unfilled squares*), 21 days (*unfilled circles*), and 45 days (*unfilled inverted triangles*). Electrodes were kept in 1.0×10^{-5} M of Cu^{2+}

All aqueous solutions were prepared from nitrate salts, while potassium and sodium salts were used for the determination of specific anion interferences. Acetic acid, ethanol, acetone, sodium hydroxide, and hydrochloric acid were provided by Kemika (Zagreb, Croatia). EDTA was obtained from Sigma Aldrich (St. Louis, MO, USA).

Common stock solutions were used for the preparation of 0.1- and 0.01-M solutions. All aqueous solutions were prepared using double-distilled water.

Potentiometric measurements

The external reference electrode was a double-junction Ag/AgCl/KCl, 3 M (Mettler Toledo InLab 301 electrode). The potentiometric measurements were carried out by means of

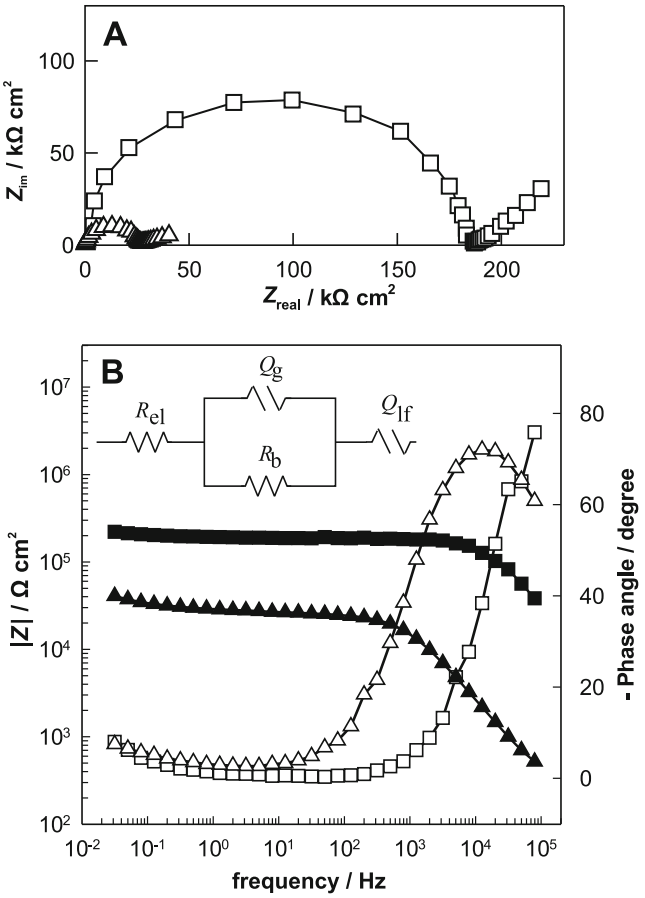

Fig. 4 Impedance spectra (Nyquist (**a**) and Bode (**b**) plots) obtained for electrodes T-1 (*unfilled squares*) and optimized T-2 electrode (*unfilled triangles*) immediately after initial contact with electrolyte. The spectra were recorded in 0.5 M KNO_3, spiked with 1.0×10^{-5} M Cu^{2+}. *Inset*, equivalent electrical circuit model used for analysis

Mettler Toledo SevenEasy pH meter, which was connected to a personal computer. The potential build-up across the membrane electrode was measured using the following electrochemical cell assembly: SC-ISE/test solution/external reference electrode. Before potentiometric measurements, electrodes were conditioned in 1.0×10^{-5} M Cu^{2+} for 24 h. The potential was recorded after addition of standard metal salt solution in magnetically stirred 0.1 M KNO_3 solution. The investigated concentration of Cu^{2+} in the sample solution ranged from 1.0×10^{-8} M to 2.8×10^{-2} M. Detection limits were estimated according to IUPAC [43] from the cross-point of the lines fitted to the linear segments of a potential vs. log a_i curve, where a_i denotes single-ion activity of the primary ion.

Impedance measurements

The experiments were carried out using a standard three-electrode electrochemical cell. The counter-electrode was a platinum electrode and the reference electrode was a saturated calomel electrode (SCE).

All measurements were carried out using a Solartron SI 1287 electrochemical interface and a Solartron SI 1255 frequency response analyzer connected to a personal computer. Impedance spectra were recorded in 0.5 M KNO_3 solution at room temperature (unless otherwise noted) within the frequency range of 100 kHz–30 mHz using 10-mV rms sinusoidal perturbation. Measurements were performed at the open circuit potential (E_{ocp}), unless otherwise noted.

Results and discussion

Potentiometric study

On the basis of the previous results [41, 44], ionophore SAPhTE was chosen for the development of a solid-contact ISE. Preliminary studies, which included covering of graphite electrode surfaces with mixtures containing different amounts of ionophore and carbon ink, did not give satisfactory results. Thus, further research was focused on carbon ink as the transducer layer and its compatibility with ion-selective polymer membranes. Three types of electrodes were developed and potentiometric results obtained for the optimized ones are shown in Fig. 2 and Table 1.

The first electrode type included only carbon ink (c) as an intermediate layer. The response of this electrode type (T-1) was characterized by strong potential drift and non-Nernstian slope (see Table 1; Fig. 2), probably induced by the undefined electric contact surface between polymer membrane and carbon ink. Therefore, this type of electrode was eliminated from further potentiometric investigation.

In order to produce a better integrated solid-contact electrode, a new layer, the carbon ink modified with polymer membrane cocktail (d) was inserted between the pure carbon ink layer (c) and the polymer membrane (e) (second electrode type, T-2). The performance of electrodes with different

Table 3 Impedance parameters for electrode T-1 and optimized T-2 electrode as determined using the equivalent circuit presented in Fig. 4

Electrode	R_{el} (Ω cm^2)	R_b (kΩ cm^2)	$Q_g\times10^{-8}$ (Ω^{-1} s^n cm^{-2})	Number, n	$Q_{lf}\times10^{-6}$ (Ω^{-1} s^n cm^{-2})	Number, n
T-1	–	191.49	0.02	0.88	50.72	0.47
T-2	10.00	24.30	1.74	0.91	110.60	0.30

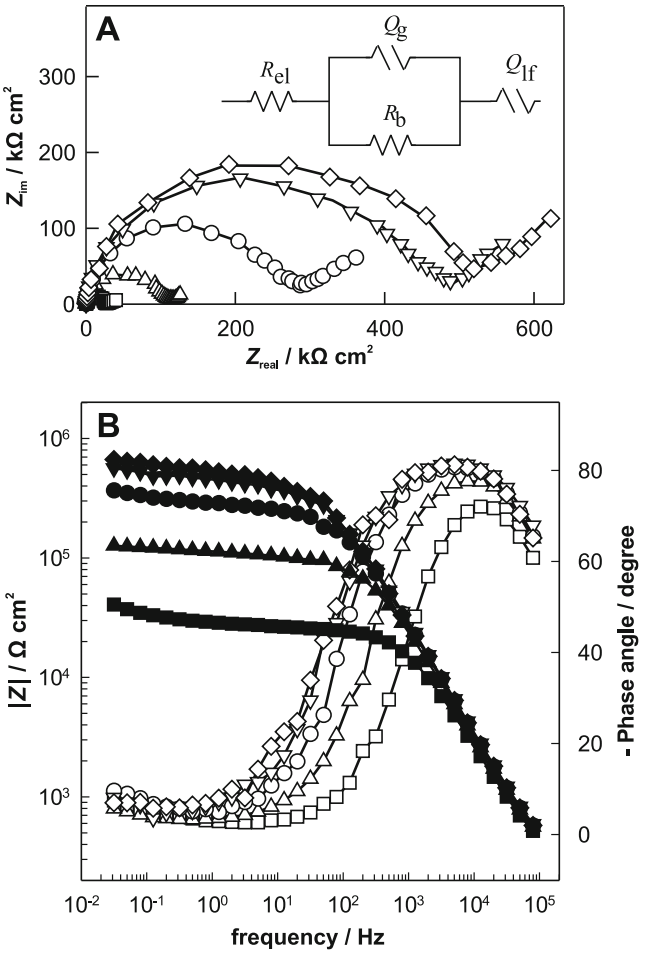

Fig. 5 Impedance spectra (Nyquist (**a**) and Bode (**b**) plots) obtained for optimized T-2 electrode over a period of 86 h: initial contact (*unfilled squares*), 4 h (*unfilled triangles*), 18 h (*unfilled circles*), 43 h (*unfilled inverted triangles*), and 86 h (*unfilled diamonds*). The electrode was kept in 0.5 M KNO_3, spiked with 1.0×10^{-5} M Cu^{2+}. *Inset*, equivalent electrical circuit model used for analysis

composition (see Table 2) of intermediate layer (d) was investigated and best results were obtained when the composition of the intermediate layer was made up of 100 mg of carbon ink and 1 ml of membrane cocktail. By using the optimized T-2 electrode, stable potential was achieved within a few seconds, and it remained mostly stable, except for a slight instability at a higher concentration of Cu^{2+}. The electrode shows a Nernstian slope (29.5 mV dec^{-1}) in the concentration range from 2.8×10^{-6} to 2.8×10^{-2} M, with detection limit of 1.8×10^{-6} M (Fig. 2). Decreasing of the amount of carbon ink resulted in the deterioration of potentiometric characteristics, which may be related to the formation of a polymer membrane film at the boundary between the intermediate layer (d) and carbon ink (c) which blocks the transfer of electrical signal.

In the third type of electrodes (T-3), intermediate layer (d), with the same composition as the optimized T-2

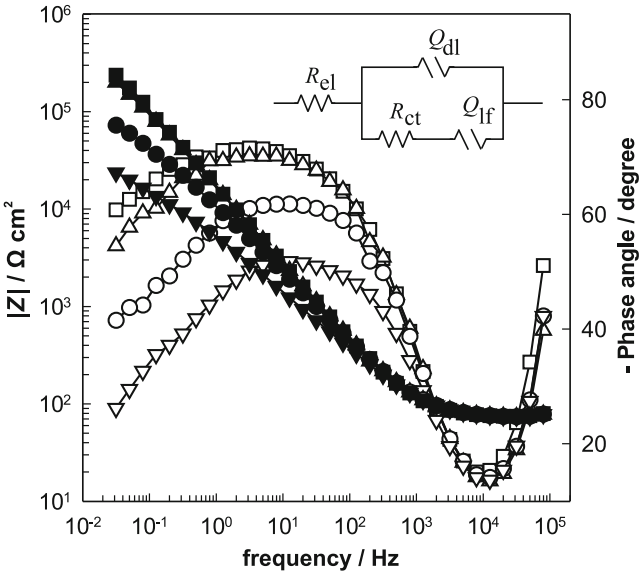

Fig. 6 Impedance spectra obtained for optimized T-3 electrode at different chatodic overpotentials: E_{ocp} (*unfilled squares*), −40 mV *vs.* E_{ocp} (*unfilled triangles*), −60 mV *vs.* E_{ocp} (*unfilled circles*), and −80 mV *vs.* E_{ocp} (*unfilled inverted triangles*). The spectra were recorded in 0.5 M KNO_3, spiked with 1.0×10^{-5} M Cu^{2+}. *Inset*, equivalent electrical circuit model used for analysis

electrode, was used as a sensing layer. Such T-3 electrode resulted in better potential stability ($\Delta E/\Delta t$), but its response time was slower than that of a T-2 electrode. Variation of the amount of polymer membrane cocktail did not produce better potentiometric characteristics: on the contrary, decreasing of the amount of polymer membrane cocktail led to the deterioration of potentiometric character-

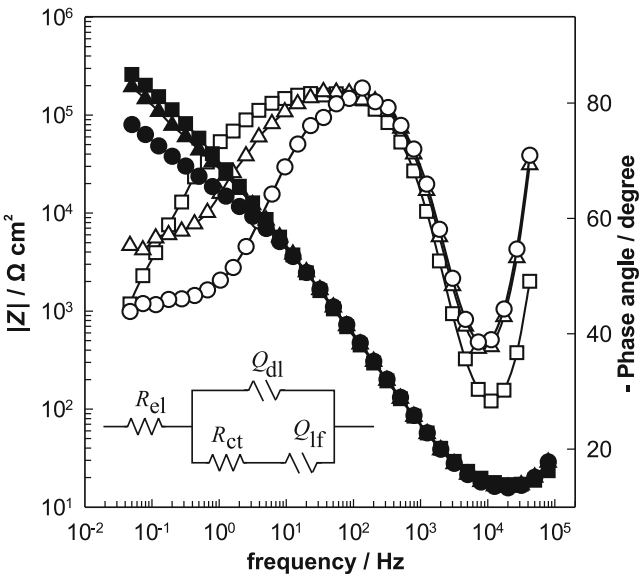

Fig. 7 Impedance spectra obtained for electrode based on pure carbon ink at different concentrations of Cu^{2+} in 0.5 M KNO_3: without (*unfilled squares*), 1.0×10^{-5} M (*unfilled triangles*), and 1.0×10^{-3} M (*unfilled circles*). *Inset*, equivalent electrical circuit model used for analysis

Table 4 Impedance parameters for optimized T-3 electrode, at different chatodic overpotentials E_{ocp}, as determined using the equivalent circuit presented in Fig. 6

E vs. E_{ocp}	R_{el} (Ω cm^2)	$Q_{lf}\times10^{-6}$ (Ω^{-1} s^n cm^{-2})	Number, n	R_{ct} (kΩ cm^2)	$Q_d\times10^{-6}$ (Ω^{-1} s^n cm^{-2})	Number, n
0 mV	71.33	13.50	0.79	1.471	–	0.5
−40 mV	69.67	15.70	0.76	203.97	13.1	0.5
−60 mV	66.45	22.70	0.72	73.84	33.3	0.5
−80 mV	61.30	43.22	0.64	39.82	155.0	0.5

istics. The optimized T-3 electrode had near-Nernstian slope (31.5 mV dec^{-1}) in the concentration range from 3.2×10^{-6} to 2.8×10^{-2} M, with detection limit of 1.6×10^{-6} M, very similar to the electrode T-2 (Fig. 2).

Potentiometric responses of T-2 and T-3 electrodes were repeatedly monitored to examine their dependence on conditioning time (in 10^{-5} M of Cu^{2+}), and these results are presented in Fig. 3. Over the course of 45 days, both types maintained satisfactory potentiometric characteristics. Afterwards, for the T-2 electrode, the penetration of electrolyte through the polymeric membrane to the intermediate layer was observed, resulting in the deterioration of potentiometric characteristics. On the other hand, the T-3 electrode was characterized by a downward drift of initial potential, but the potentiometric characteristics remained unchanged. When electrodes were kept in a dry place, their lifetime was significantly improved (3 and 5 months for T-2 and T-3, respectively).

Impedance study

Further characterization for all three types of electrodes was carried out by electrochemical impedance spectroscopy. Impedance spectra, obtained for T-1 and optimized T-2 electrodes and presented in Fig. 4, were fitted with an equivalent electrical circuit shown in the inset of Fig. 4, and the results of this fitting are given in Table 3.

Both types of electrode show a similar pattern with a high-frequency semicircle arising from the bulk resistance R_b of the polymer membrane in parallel with its geometrical capacitance (C_g), represented by parameters n and Q_g of constant phase element. The low-frequency region reveals a component which is probably related to ion diffusion, to and through the membrane.

The bulk membrane resistance should be the same for both electrode types, but the observed differences in R_b are too high (191.5 and 24.3 kΩ for T-1 and optimized T-2 electrodes, respectively), thus excluding the reasons related to the reproducibility of electrode preparation (variation in polymer membrane thickness) as a potential explanation. According to Veltsistas et al. [27] a phenomenon at the interface between the solid contact and the polymer membrane is not clearly defined due to the diffusion of the polymer membrane solution into the highly porous graphite ink.

However, this explanation does not fit our results since a higher value of bulk resistance is expected for the electrode T-2 if we assume facilitated penetration of the polymer membrane into the modified CI compared to the unmodified CI. This behavior should increase the overall thickness of the membrane and therefore increase the bulk resistance. Del Marco et al. [45] have shown that a high-frequency resistance does not represent only bulk membrane resistance but also convoluted contact resistance at the solid contact/ISE membrane buried interface coupled with the bulk membrane resistance (named bulk membrane contact resistance). So, in our case, the likely explanation is that the incorporation of modified CI facilitates the transformation from ionic to electron conductivity due to a larger contact area between the graphite particles and the membrane bulk. The abovementioned event probably causes a higher value, at two orders of magnitude, of C_g for the T-2 electrode compared to T-1, which correlates with a stable potentiometric response.

Previous EIS studies [46, 47] have shown that bulk membrane contact resistance exhibits a diminution when the solid-contact ISE is exposed to an aqueous electrolyte for a prolonged period of time. Accordingly, EIS provides a sensitive electrochemical technique for probing the water layers in solid-contact ISEs since even localized repositories of water are formed at pores and pinholes, enabling detection by this technique. Impedance spectra obtained

Table 5 Impedance parameters for electrode based on pure carbon ink, at different concentrations of Cu^{2+}, as determined using the equivalent circuit presented in Fig. 7

c (Cu^{2+}) (M)	R_{el} (Ω cm^2)	$Q_{lf}\times10^{-6}$ (Ω^{-1} s^n cm^{-2})	Number, n	R_{ct} (kΩ cm^2)	$Q_d\times10^{-6}$ (Ω^{-1} s^n cm^{-2})	Number, n
0	13.50	5.90	0.89	364.56	–	–
1.0×10^{-5}	12.47	4.42	0.92	22.35	7.89	0.5
1.0×10^{-3}	12.17	4.10	0.93	8.37	23.07	0.5

Table 6 Selectivity coefficients for optimized T-2 and T-3 electrodes determined by MPM

Interferent (B)	$K^{pot}_{Cu^{2+},B}$	
	Type of electrode	
	T-2	T-3
Pb^{2+}	3.9×10^{-3}	1.0×10^{-2}
Zn^{2+}	2.5×10^{-3}	5.1×10^{-3}
Mn^{2+}	7.9×10^{-4}	2.3×10^{-3}
Cd^{2+}	9.2×10^{-4}	8.2×10^{-5}
Fe^{2+}	3.1×10^{-5}	1.0×10^{-5}
Co^{2+}	1.0×10^{-6}	1.0×10^{-5}
Na^{+}	$>1.0\times10^{-7}$	$>1.0\times10^{-7}$
K^{+}	$>1.0\times10^{-7}$	$>1.0\times10^{-7}$
Ca^{2+}	$>1.0\times10^{-7}$	$>1.0\times10^{-7}$
Ni^{2+}	$>1.0\times10^{-7}$	$>1.0\times10^{-7}$
Ag^{+}	$>1.0\times10^{-7}$	$>1.0\times10^{-7}$

during soaking of optimized T-2 electrode in 0.5 M KNO_3 spiked with 1.0×10^{-5} Cu^{2+} are shown in Fig. 5. A high-frequency semicircle, which represents bulk membrane contact resistance, shows the increase in impedance, indicating that drop-casting of PVC membrane on the modified intermediate carbon ink layer prevented the formation of a pernicious water layer. Increasing of R_b can be attributed to the intake of water, drawing ions or charged ions out of the continuous membrane into pockets of isolated water [48]. During performed water layer test according to IUPAC [49], no potential drift was observed for electrodes in discriminating solution (results not shown); the final replacement of the test solution by the original solution gives rise to an almost null negative potential drift.

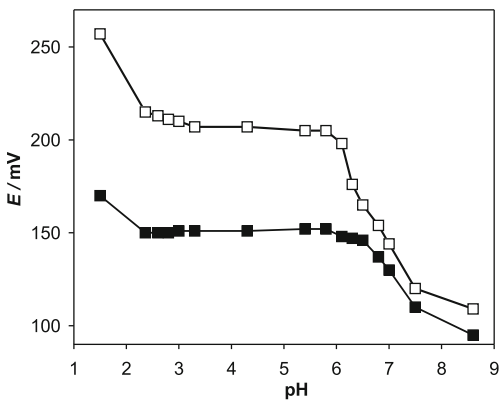

Fig. 8 The effect of pH of the test solution on the potentiometric response of the optimized T-2 (*filled squares*) and T-3 (*unfilled squares*) electrodes at 1.0×10^{-3} M of Cu^{2+}

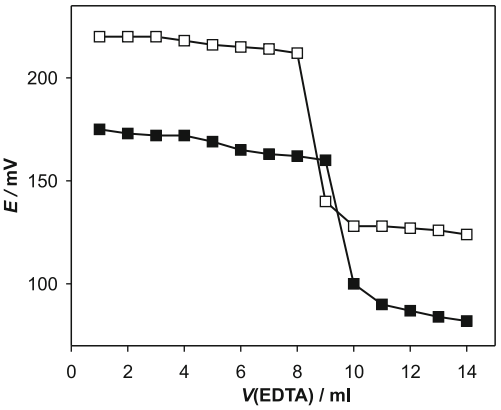

Fig. 9 The potentiometric titration plots of 30 ml of 3.0×10^{-3} M of Cu^{2+} against EDTA (0.01 M), using the optimized T-2 (*filled squares*) and T-3 (*unfilled squares*) electrodes as indicator electrodes, at pH=5.5

Impedance spectra, obtained with T-3 electrode at different cathodic overpotentials in 1.0×10^{-5} M Cu^{2+} solution, and spectra obtained on the pure carbon ink electrode (without its modification with polymer membrane cocktail) in the solution with different Cu^{2+} concentration are presented in Figs. 6 and 7, respectively. The data were fitted with the equivalent electrical circuit, shown in the inset of Fig. 6, and the results of this fitting procedure are given in Tables 4 and 5. A similarity of these spectra can be noticed, which is not surprising, keeping in mind the construction of the electrodes. The value of R_{ct} decreases with an increase of cathodic overpotential and increases with a decrease of Cu^{2+} concentration. These results are in accordance with the reaction mechanism for Cu^{2+} reduction

Table 7 Comparison of various reported Cu(II) ISE with the present work

Type	Slope (mV dec^{-1})	Detection limit/M	Response time/s	Reference
CPE	29.6	7.9×10^{-7}	15	[34]
CPE	31.1	4.1×10^{-9}	–	[40]
PME	27.0	5.1×10^{-7}	5	[41]
PME	29.4±0.5	8.0×10^{-6}	15	[52]
CPE	30.0±2.0	7.0×10^{-7}	45	[53]
CGE	29.1±0.1	3.0×10^{-8}	5	[54]
CWE	28.2	5.0×10^{-7}	10–50	[55]
CWE	29.0	1.0×10^{-6}	10–15	[56]
CWE	29.5±1.6	9.8×10^{-8}	9	[57]
SC	29.5	1.8×10^{-6}	5	This work
SC	31.0	1.6×10^{-6}	10	This work

CPE carbon paste electrode, *CWE* coated wire electrode, *CGE* coated graphite electrode, *PME* polymer membrane electrode with internal liquid contact, *SC* polymer membrane electrode with internal solid contact

[50]. So, it can be concluded that in T-3 electrode design, the graphite network itself acts as electronic conductor.

Selectivity and pH dependence

Selectivity is one of the most important characteristics of the sensor, as reflected in the relative response of the sensor for the primary ion in the presence of the other interfering ions. The selectivity coefficients obtained for proposed electrodes using the match potential method (MPM) [51] are summarized in Table 6. The selectivity coefficient indicates that the potentiometric determination of the Cu^{2+} will not be disturbed by the presence of the examined ions. The interference of anions has also been researched as halides are known to cause interference in the determination of Cu^{2+}. No interference was noticed with the examined anions: SO_4^{2-}, CH_3COO^-, salicylate, Br^-, Cl^-, phosphate, NO_3^-, and SCN^-. However, a strong interference was observed in the presence of Hg^{2+}, which was expected, bearing in mind our previous works [41, 44].

The pH dependence of the electrodes' potential was examined in the presence of 1.8×10^{-3} M of Cu^{2+} over a wide pH range of 1–9 by the addition of appropriate amounts of HNO_3 and NaOH. For the optimized T-2 and T-3 electrodes, the results are depicted in Fig. 8. The potential remained constant over the pH range between 2.3–6.5 and 2.3–6.1 for electrodes T-2 and T-3, respectively, which may be taken as the working range of the electrode. The drift of the potential at pH lower than 2.3 can be attributed to the interference of H^+ ions, which is due to the high rate of diffusion from the sample to a membrane phase and the interaction with ionophore (protonation). A potential decrease was observed at pH higher than 6.5 (6.1) due to the formation of hydroxyl complexes of Cu^{2+} in the solution and finally the precipitation of $Cu(OH)_2$ (s).

Analytical chemistry applicability

The analytical chemistry applicability was evaluated by the potentiometric titration of Cu^{2+} with EDTA. The amount of 30 ml of 1.3×10^{-3} M Cu^{2+} solution was titrated against 1.0×10^{-2} M EDTA. The obtained titration plots for both proposed electrodes are shown in Fig. 9. As it can be seen, electrodes can be used for the determination of Cu^{2+} by potentiometric titration with EDTA.

Comparison of the proposed electrodes with other Cu^{2+} ion-selective electrodes

The characteristic responses of optimized T-2 and T-3 electrodes and other ion-selective electrodes are listed in Table 7. From the results in this table, it can be concluded that these electrodes are comparable to previously reported electrodes in most cases.

Conclusions

In our work, two types of solid-contact potentiometric sensors were developed using commercial carbon ink and polymer membrane with SAPhTE as ionophore. Based on the results presented earlier, it can be concluded that potentiometric characteristics strongly depend on the composition of an intermediate layer.

When carbon ink is used as the intermediate layer itself, the potentiometric response is characterized by instability and loss of sensitivity. Incorporation of a novel layer, consisting of carbon ink modified with a polymer membrane cocktail, between carbon ink and polymer membrane probably provides a smoother transition between the two bulk materials, which results in significant improvements with regards to electrode potentiometric characteristics. Impedance measurements revealed that such modification of carbon ink decreases the bulk contact resistance of the transducer layer and the polymer membrane and thus facilitates transformation from ion to electron conductivity.

Also, satisfactory potentiometric characteristics for carbon ink composite polymer–membrane electrode (T-3 electrode) were obtained and a significant influence of carbon network on electrical properties was confirmed by impedance measurements.

The potentiometric characteristics obtained, together with low cost and easy preparation, make these solid contact electrodes very promising sensors for the determination of Cu(II) ions.

References

1. Bakker E, Diamond D, Lewenstam A, Pretsch E (1999) Anal Chim Acta 391:11–18
2. Pretsch E, Trends (2007) Anal Chem 26:46-51
3. Cattrall RW, Freiser H (1971) Anal Chem 43:1905–1906
4. Cattrall RW, Drew DW, Hamilton IC (1975) Anal Chim Acta 76:269–277
5. Liu D, Meruva RK, Brown RB, Meyerhoff ME (1996) Anal Chim Acta 321:173–183
6. Sutter J, Radu A, Peper S, Bakker E, Pretsch E (2004) Anal Chim Acta 523:53–59
7. Pandey PC, Prakash R (1998) Sens Actuators B 46:61–65
8. Lindfors T, Sjöberg P, Bobacka J, Lewenstam A, Ivaska A (1999) Anal Chim Acta 385:163–173
9. Marques de Oliveira IA, Pla-Roca M, Escriche L, Casabó J, Zine N, Bausells J, Teixidor F, Crespo E, Errachid A, Samitier J (2006) Electrochim Acta 51:5070–5074
10. Zine N, Bausells J, Teixidor F, Viñas C, Masalles C, Samitier J, Errachid A (2006) Mat Sci Eng C 26:399–404

11. Ocypa M, Michalska A, Maksymiuk K (2006) Electrochim Acta 51:2298–2305
12. Gyurcsanyi RE, Rangisetty, Clifton N, Pendley BD, Lindner E (2004) Talanta 63:89-99
13. Grygolowicz-Pawlak E, Plachecka K, Brzózka Z, Malinowska E (2007) Sens Actuators B 123:480–487
14. Grygołowicz-Pawlak E, Wyglądacz K, Sęk S, Bilewicz R, Brzózka Z, Malinowska E (2005) Sens Actuators B 111:310–316
15. Fibbioli M, Bandyopadhyay K, Liu SG, Echogoyen L, Enger O, Diederich F, Buhlmann P, Pretsch E (2000) Chem Commun 5:339–340
16. Martínez-Barrachina S, Alonso J, Matia L, Prats R, del Valle M (2001) Talanta 54:811–820
17. Isildak I (2000) Turk J Chem 24:389–394
18. Puig-Lleixà C, Jiménez C, Fàbregas E, Bartrolí J (1998) Sens Actuators B 49:211–217
19. Górski L, Matusevich A, Pietrzak M, Wang L, Meyerhoff ME (2009) J Solid State Electroc 13:157–164
20. Gismera MJ, Sevilla MT, Procopio JR (2007) Talanta 74:190–197
21. Abbaspour A, Mirahmadi, Khalafi-Nezhad EA, Babamohammadi S (2010) J Hazard Mater 174:656–661
22. Abbaspour A, Refahi M, Khalafi-Nezhad A, Soltani Rad N, Behrouz S (2010) J Hazard Mater 184:20–25
23. Koncki R, Głąb S, Dziwulska J, Palchetti I, Mascini M (1999) Anal Chim Acta 385:451–459
24. Mohamed GG, Ali TA, El-Shahat MF, Al-Sabagh AM, Migahed MA, Khaled E (2010) Anal Chim Acta 673:79–87
25. Khaled E, Mohamed GG, Awad T (2008) Sens Actuators B 135:74–80
26. Khaled E, Hassan HNA, Girgis A, Metelka R (2008) Talanta 77:737–743
27. Veltsistas PG, Prodromidis MI, Efstathiou CE (2004) Anal Chim Acta 502:15–22
28. Crespo GA, Macho S, Rius X (2008) Anal Chem 80:1316–1322
29. Crespo GA, Macho S, Bobacka J, Rius X (2009) Anal Chem 81:676–681
30. Ganjali MR, Khoshsafar H, Shirzadmehr A, Javanbakht M, Faridbod F (2009) Int J Electrochem Sci 4:435–443
31. Faridbod F, Ganjali MR, Larijani B, Norouzi P (2009) Electrochim Acta 55:234–239
32. Khani H, Rofouei MK, Arab P, Gupta VK, Vafaei Z (2010) J Hazard Mater 183:402–409
33. Peng B, Zhu J, Liu X, Qin Y (2008) Sens Actuators B 133:308–314
34. Ganjali MR, Poursaberi T, Khoobi M, Shafiee A, Adibi M, Pirali-Hamedani M, Norouzi P (2011) Int J Electrochem Sci 6:717–726
35. Ganjali MR, Motakef-Kazami N, Faridbod F, Khoee S, Norouzi P (2010) J Hazard Mater 17:415–419
36. Ahuja T, Kumar D, Singh N, Biradar AM, Rajesh (2010) Mat Sci Eng C 31(2011):90–94
37. Mashhadizadeh MH, Khani H (2010) Anal Methods 2:24–31
38. Mashhadizadeh MH, Khani H, Foroumadi A, Sagharichi P (2005) Anal Chim Acta 665:208–214
39. Mashhadizadeh MH, Khani H, Shochravi A (2010) J Incl Phenom Macrocycl Chem 68:219–227
40. Mashhadizadeh MH, Eskandari K, Foroumadi A, Shafiee A (2008) Talanta 76:497–502
41. Brinić S, Buzuk M, Generalić E, Bralić M (2010) Acta Chim Slov 57:318–324
42. Rajsekhar G, Rao CP, Saarenketo PK, Kolehmainen E, Rissanen K (2002) Inorg Chem Comm 5:649–652
43. Buck RP, Lindner E (1994) Pure Appl Chem 66:2527–2536
44. Buzuk M, Brinić S, Generalić E, Bralić M (2009) Croat Chem Acta 82:801–806
45. Marco R, Jee E, Prince K, Pretsch E, Bakker E (2009) J Solid State Electrochem 13:137–148
46. Marco R, Veder JP, Clarke G, Nelson A, Prince K, Pretsch E, Bakker E (2008) Phys Chem Chem Phys 10:73–76
47. Chester RT (2007) Thesis, Curtin University of Technology, Perth, Australia
48. Horvai G, Graf E, Toth K, Pungor E, Buck RP (1986) Anal Chem 58:2735–2740
49. Lindner E, Umezawa Y (2008) Pure Appl Chem 80:85–104
50. Krzewska S (1997) Electrochim Acta 42:3531–3540
51. Umezawa Y, Bühlmann P, Umezawa K, Tohda K, Amemiya S (2000) Pure Appl Chem 2:1851–2082
52. Shamsipur M, Javanbakht M, Mousavi MF, Ganjali MR, Lippolis V, Garau A, Tei L (2001) Talanta 55:1047–1054
53. Abbaspour A, Moosavi SMM (2002) Talanta 56:91–96
54. Ganjali MR, Poursaberi T, Haji-agha Babaei L, Rouhani S, Yousefi M, Kargar-Razi M, Moghimid A, Aghabozorg H, Shamsipur M (2001) Anal Chim Acta 440:81–87
55. Firooz AR, Mazloum M, Safari J, Amini MK (2002) Anal Bioanal Chem 372:718–722
56. Ardakani MM, Mirhoseini SH, Salavati-Niasari M (2006) Acta Chim Slov 53:197–203
57. Shokrollahi A, Abbaspour A, Ghaedi M, Naghashian Haghighi A, Kianfar AH, Ranjbar M (2011) Talanta 84:34–41